LIDAR STUDIES OF MARITIME CLOUDINESS

G.P. Kokhanenko, I.E. Penner, and V.S. Shamanaev

Institute of Atmospheric Optics,
Siberian Branch of the Russian Academy of Sciences, Tomsk

Received June 10, 1996

The low cloud boundary has been investigated with a lidar placed onboard a scientific vessel sailed in the North Atlantic. Its height is 0.1–5.5 km. *It has been found that the heights of low boundaries of stratiform cloud cells* 5–70 km *long obey the asymmetric distribution rather than the Gaussian one. The coefficient of asymmetry may be positive or negative. The laser radiation extinction coefficient also obeys the asymmetric distribution in most cases.*

Interest to a study of clouds is conditioned by their continuous impact on the weather. Whereas ground-based lidars have long been in use and cloud measurements are relatively regular, the data on maritime clouds are very scarce. Since oceans occupy about 70% of the global area, one can appreciate the interest with which the Institute of Atmospheric Optics accepted a proposal of the Institute of Oceanography of the Russian Academy of Sciences to take part in the 37th mission of the scientific-research vessel *Academician Mstislav Keldysh*.

Experiments were performed in the Atlantic, when the vessel sailed along 50°N as well as in the Barents, Norwegian, and North seas in August–October of 1995. We worked on the periphery of highs and lows not only under fine weather conditions with a small cloud amount, but also under stormy weather conditions when the cloud cover index reached 10.

The measurements were performed with the Makrel'-2 lidar,[1] in which the optical axes of a transmitter and a receiver were collocated to place the lidar into a cabin and to bring a laser beam out of the vessel after its reflection from an inclined mirror of limited size. The mirror was oriented so as not to distort the parameters of a linearly polarized sounding pulse and lidar return signal characteristics.[2] Output analog signals from the FÉU-84-3 photomultipliers were digitized by the ATP 7.100 7-bit analog-to-digital converter (ADC) whose sampling time varied from 10 to 320 ns.

Measurements were performed every day in the course of 10 weeks, and the measurement run lasted from 10 min to 1.5 h for a pulse repetition frequency of 1 Hz. The velocity of the vessel and the wind velocity at an altitude of 18 m above the water surface were measured independently. In the first approximation, it was assumed that clouds drifted with the wind velocity.

We measured the following parameters of the low cloud boundary (LCB) structure: height of the LCB, its extinction coefficient, and depolarization ratio. It is well known[3] that the LCB is the transitive layer whose thickness is about several tens of meters. Its properties may change regularly or may fluctuate (within 10–100 m) as functions of the relationships among the dew-point deficit, turbulent exchange coefficient, vertical temperature gradient, and the vertical wind velocity component.

Several criteria of lidar determination of the LCB height were considered in Ref. 4. In the present paper, we used two of them based on an analysis of lidar return signal derivative. The LCB height was determined as a distance r_0 to the point at which the signal just started to increase when the lidar beam after its propagation through the clear air atmosphere entered the cloud itself or as a distance $r_{\rm m}$ to the point at which the lidar return signal maximized.

In computer processing of lidar signal arrays, a problem of formalization of the chosen criteria arises, in our case, of r_0 and $r_{\rm m}$, because clouds are often inhomogeneous and a series of local extrema occurs in a lidar return signal. Additional error is introduced due to noise of different origin, and so on. In the present paper, $r_{\rm m}$ was determined as the distance to the point that lies outside the near field of the lidar at which a signal reached a level of $1/e = 0.37$ of the absolute signal maximum. To eliminate the effect of signal fluctuations in the region of signal minimum, r_0 was determined as follows. In the region between the near field of the lidar and $r_{\rm m}$, the point of the absolute signal minimum was found. Then three signal counts were sampled with the sampling step of the ADC to the right of this minimum. If the amplitudes of these three counts were greater than the absolute minimum amplitude plus the error of background measurements, this point would be taken as r_0. Otherwise, the procedure was repeated with the point shifted by one count to the right. We note that the roll angles were 3–5°, as a rule. This introduced additional error of 0.1–0.3% in the measured LCB height. Under conditions of storms, when the roll angles reached 8°, this error increased up to 1%.

The extinction coefficient $\varepsilon(r)$ at a distance r from the lidar was calculated from the lidar return signal power $P(r)$ by the following formula:

0235-6880/96/10 888-07 $02.00

$$\varepsilon(r) = \frac{1}{2}\,\frac{P(r)r^2}{\int\limits_{r_0}^{r_\infty} P(x)x^2\,\mathrm{d}x - \int\limits_{r_0}^{r} P(x)x^2\,\mathrm{d}x}\,. \qquad (1)$$

Here, r_∞ is the maximum range of lidar operation from which a lidar return signal is still recorded. The condition of applicability of the above asymptotic formula is $\int\limits_{r_0}^{r_\infty} \varepsilon(x)\,\mathrm{d}x \geq 3$.

The radiation extinction coefficient at the cloud boundary ε_b was defined[4] as the value of $\varepsilon(r)$ averaged along the laser beam propagation path when the depth of laser beam penetration into the cloud was equal to half the distance of signal accumulation, i.e.,

$$\varepsilon_\mathrm{b} = \frac{2}{r_\infty - r_0} \int\limits_{r_0}^{(r_0 + r_\infty)/2} \varepsilon(x)\,\mathrm{d}x\,. \qquad (2)$$

For subsequent analysis, experimental data were divided into two groups: the first data array with the LCB heights up to 600–800 m characterized by strong interaction with the sea surface, and the second data array with the LCB heights from 1.5 to 6 km, for which this interaction was much weaker. (In principle, there are several criteria of preliminary classification.) Situations in which the LCB merges with the sea, or a dense fog is presented, or the LCB is masked by precipitation will be considered further, because in these cases the notion "the cloud boundary" ceases to have its conventional meaning.

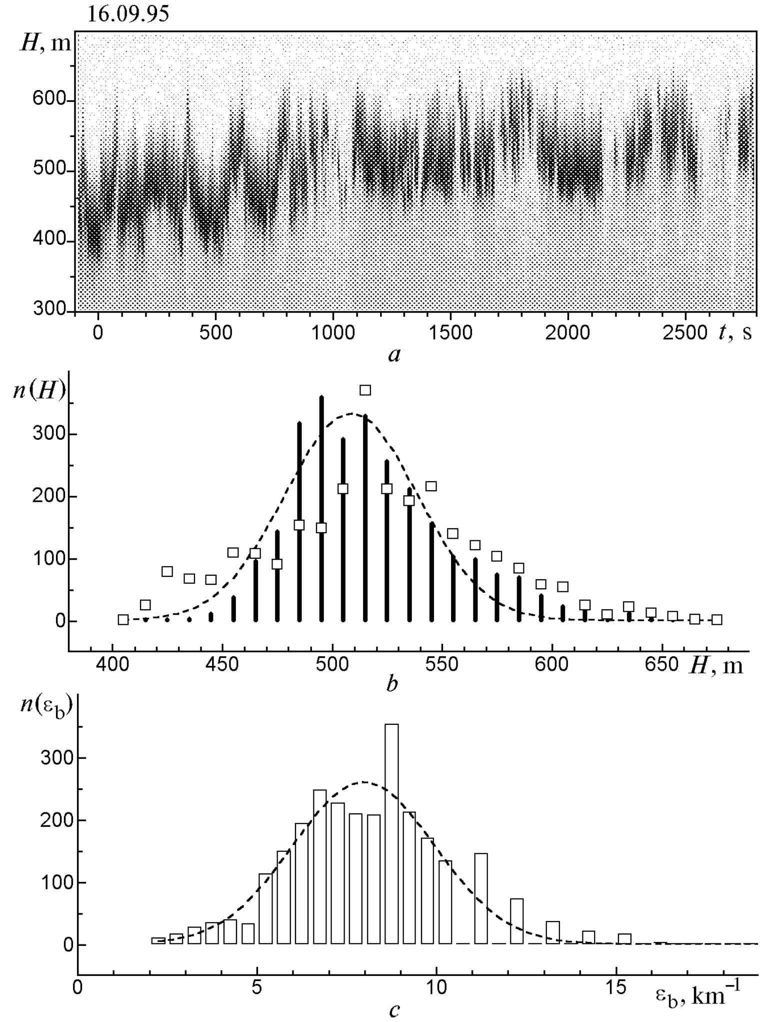

FIG. 1. Sensing of stratocumulus clouds at 16:10*, ship time on September 16, 1995: echogram of 2653 lidar return signals in coordinates "time from the start of measurement run – altitude above the sea surface" (case a); histograms of n(H) (empirical probability distribution function of the LCB height H (case b); histogram n(ε_b) of the distribution of the extinction coefficient ε_b at the LCB (case c). In Fig. 1b small squares are for the initial data array, vertical bars denote n(H) after elimination of the trend, dashed curve is for the Gaussian approximation of n(H). In Fig. 1c, vertical bars show the histogram of the distribution n(ε_b) and the dashed curve is for the Gaussian approximation of n(ε_b).*

Now we consider some particular realizations of signals and their generalized characteristics. Thus, Fig. 1 shows the result of sensing of stratocumulus clouds on September 16, 1995 (in the gaps, high stratified clouds were seen at an altitude of 2800 m). Here, Fig. 1*a* shows the time history of lidar return signal intensities on scale of grey: the larger is the signal intensity, the higher is the degree of blackening, as functions of the altitude plotted on the ordinate. The totality of 2653 lidar return signals is shown in this figure. Considering the above assumption about the wind speed and direction, the spatial extension of this record is 42 km. In this case, the LCB height increased steadily and was equal to $H = (518 + 0.04\ t)$ m, where t is time, in sec, counted off from the start of measurement run (or the number of lidar shots at a lidar pulse repetition frequency of 1 Hz). The LCB height was calculated by the criterion of signal maximum ($H = r_\mathrm{m}$), and its standard deviation was $\Delta H = 47$ m. After elimination of the linear trend from this signal sample with the use of standard procedure, we derived $\Delta H_0 = 36$ m.

Figure 1*b* shows the empirical probability function $n(H)$ of the given LCB height H for the examined measurement run (small squares denote the initial data and vertical bars denote the probability values after elimination of the trend). It is seen that the $n(H)$ distribution is rather wide; the spread in the values of the LCB height is 200 m. The value of the asymmetry coefficient[5] was large: $As = 0.8$ when we did not eliminate the trend in the data, that is, the $n(H)$ distribution is asymmetric about its modal value H_mod and $H > H_\mathrm{mod}$ are more often encountered than $H < H_\mathrm{mod}$.

The coefficient of excess E of the distribution $n(H)$, being the measure of its peaking, was equal to 0.57 in this case. According to classification of Ref. 6, this distribution has a flattop peak, that is, it differs not too much from the normal distribution.

After elimination of the trend, $As = 0.08$ and $E = -0.14$. For the normal distribution of the measured parameters, the standard deviations of As and E depend only on the sample size, and

$$\Delta As = \sqrt{\frac{6(n_0 - 1)}{(n_0 + 1)\ (n_0 + 3)}}\ ,$$

$$\Delta E = \sqrt{\frac{2n_0(n_0 - 2)\ (n_0 - 3)}{(n_0 + 1)^2\ (n_0 + 3)\ (n_0 + 5)}}\ .$$

In accordance with Ref. 6, the distribution $n(H)$ can be considered normal when inequalities $|As| \le 3\Delta As$ and $|E| \le 5\Delta E$ hold true. In case shown in Fig. 1, $3\Delta As = 0.143$ and $5\Delta E = 0.13$, that is, the high-frequency fluctuations of the LCB (after elimination of the trend) can be considered to obey the normal distribution, as for many aerosol processes in the atmosphere.

The distribution $n(\varepsilon_\mathrm{b})$ of the extinction coefficient calculated by formula (2) is shown in Fig. 1*c*. Our estimates have shown that to the right of the modal value of ε, there are 25% of all ε_b, whereas to the left of it there are 30% of ε_b (whose values are less than the modal value) if we consider the distribution half-width.

Figure 2 shows the results of sensing of lower cloudiness. In the figure, the trend of the LCB is also manifested, and $H = (188-0.03\ t)$ m. Visually, there were stratocumulus clouds and the Moon was seen through them. (The lowest cloud layer vanished within 30 min after the completion of this measurement run, and we investigated clouds with $H_\mathrm{LCB} = 570$ m.) Figure 2*a* shows the LCB profile by the criterion r_m. The standard deviation prior to elimination of the trend was $\Delta H = 25$ m, and after elimination of the trend $\Delta H_0 = 14$ m. The sample length was estimated to be 26 km.

Figure 2*b* shows the histograms of $n(H)$ prior to (small squares, the distribution is distinctly binomial with $As = 0.64$ and $E = 2.0$) and after elimination of the trend ($As = -0.01$ and $E = -0.68$). In this case, $\Delta As = 0.056$ and $\Delta E = 0.032$ and hence $n(H)$ cannot be considered as Gaussian: it is flatter.

As to the distribution of ε_b, it is markedly asymmetric in this case. Its half-width is 16% from the modal values ε_mod toward greater values of ε_b and 42% toward smaller ones.

On the whole, for the totality of stratiform clouds with the LCB heights below 1 km we obtained the following. When the LCB had the trend, its running average height could be written as $m = m_0 \pm \mu l$, where l is the distance from the initial point of measurements and $\mu = (3.4 \pm 0.7)\cdot 10^{-3}$ (assuming that the mean wind velocity at the lower cloud boundary was 10 m/s). The maximum distance l was estimated to be 5–40 km. (Hereafter we give the standard deviations of the measured parameters.)

The spread of the LCB heights changed from 25 to 56 m in the course of experiments with a standard deviation of (39 ± 14) m, i.e., the average variation coefficient was 36% in the case of the trend. When the trend was eliminated, the spread of the LCB heights was 10–42 m with a standard deviation of (23 ± 12) m, that is, the average variation coefficient was 52%.

The coefficient of asymmetry of the distribution $n(H)$ with the trend was negative in 40% of all cases and $As = -(0.36 \pm 0.49)$, that is, had moderate absolute value. Its limiting values changed from −0.01 to −0.70, In about 60% of experiments we recorded positive coefficients of asymmetry of the "conventional" type and $As = (0.51 \pm 0.25)$, that is, the coefficient of asymmetry slightly exceeded its moderate value, and the asymmetry was stronger at the upper limit. In the limiting cases, As changed from 0.33 to 0.80.

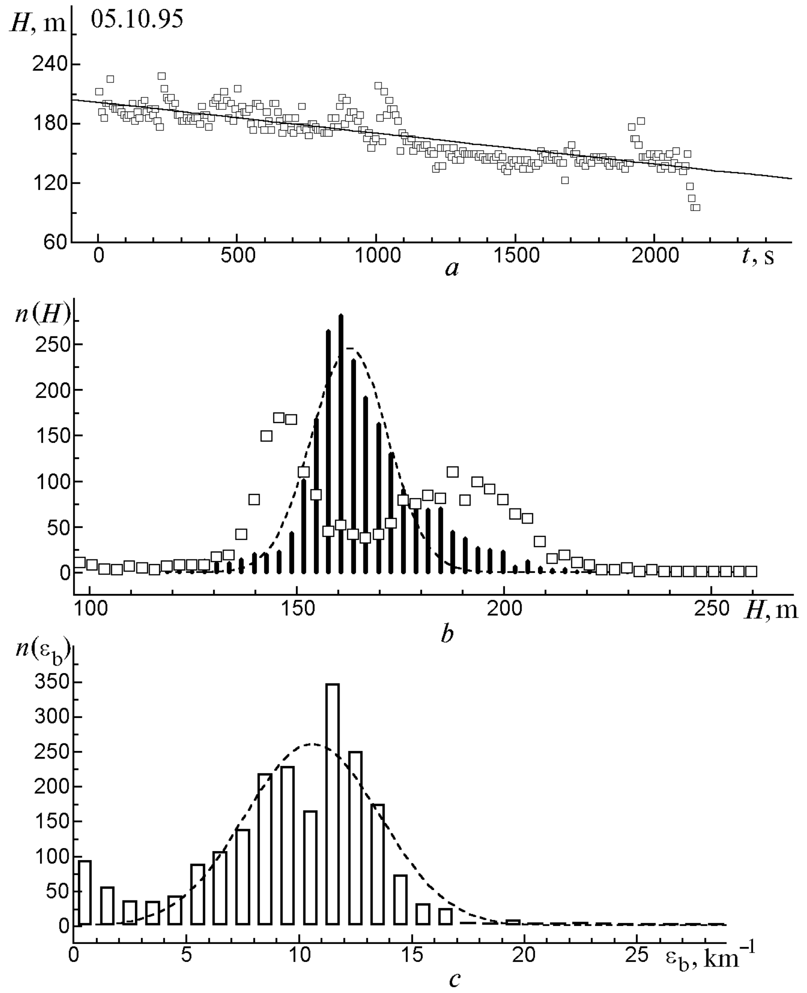

FIG. 2. Sensing of stratocumulus clouds at 20:02, ship time on October 5, 1995: the horizontal profile of the LCB by the criterion $r_{\rm m}$ (case a). Designations in cases b and c are the same as in Fig. 1.

After elimination of the trend, the distribution $n(H)$ symmetrized as a whole. Weakly pronounced asymmetry was observed in less than 20% of all cases and $As = -0.2$. In the remaining cases the asymmetry was weak or moderate and $As = (0.27 \pm 0.20)$.

The excess coefficient characterizes the degree of distribution peaking, and $E < 0$ in about 40% of cases of the LCB with the trend (distributions were flatter than the Gaussian curves), with $E = -(0.38 \pm 0.42)$. In these cases, the distribution $n(H)$ differed not too much from the normal one. For positive excess coefficient values $E = (1.83 \pm 1.40)$, that is, on the upper limit, these distribution functions were classified among sharply peaked ones. After elimination of the trend, already 40% of the excess coefficient values were positive and $E = (1.73 \pm 0.39)$. On the upper limit the distribution functions sharply peaked.

An example of sensing of relatively high clouds on September 19, 1995 is shown in Fig. 3 (rare cumulus clouds of fine weather were recorded at an altitude of 300 m). We investigated cloud fields 50–70 km long, because the wind velocity or the velocity of air jets at these altitudes often reached 50–70 m/s and even much more. In spite of the great altitude, the clouds consisted of water droplets, because their depolarization ratio did not exceed several percent.[2] This is easily explicable,because the air temperature at the sea level was 19°C, and for a standard temperature lapse rate of 6 deg/km its value at the LCB height was as low as only −14°C. This is the temperature typical of a supercooled water droplet. In this case, we did not establish any trend in the LCB behavior, and $H = (5520 \pm 108)$ m. However, an analysis of the function $n(H)$ shown in Fig. 3*b* indicates that it obeys bimodal distribution. Indeed, the lower cloud sublayer (a beard) was always recorded 300–500 m under the basic cloud layer. Here, $As = -1.18$ and $E = 2.28$.

The distribution of $\varepsilon_{\rm b}$ was asymmetric, with the increased probability of $\varepsilon_{\rm b} = 1.7$ km^{-1} that can be considered as an open question and the modal value $\varepsilon = 2$ km^{-1}.

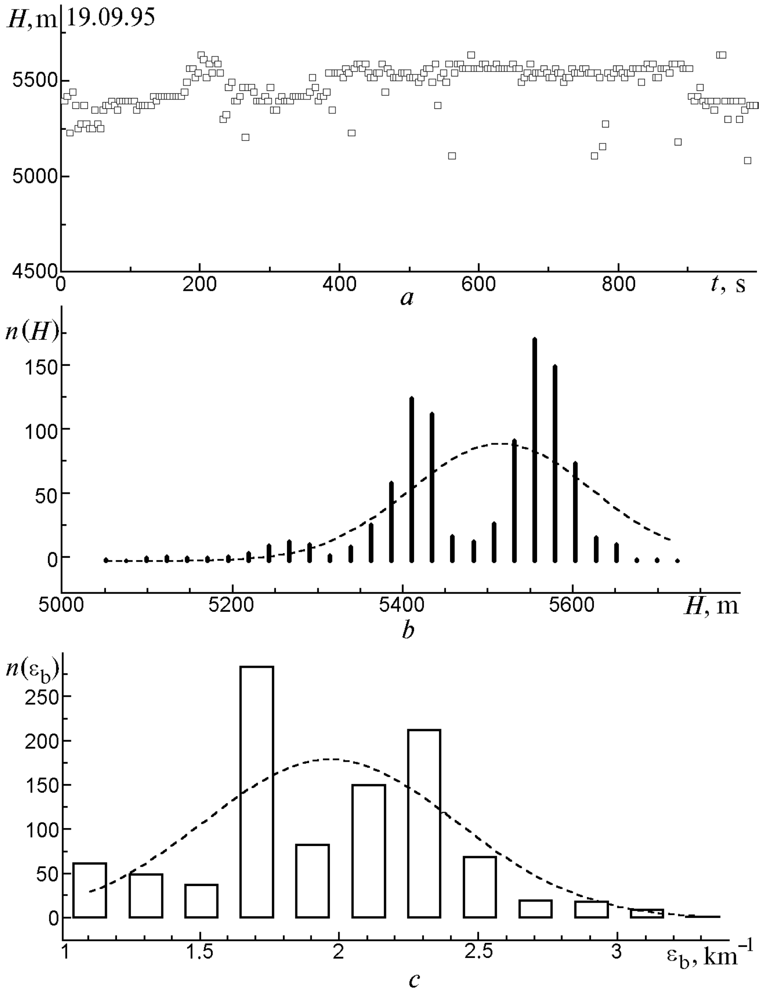

FIG. 3. Sensing of high stratified clouds at 06:57, *ship time on September 19, 1995. Designations are the same as in Fig. 2.*

Whereas the above-discussed experimental example illustrates the distribution functions that are not so apparent, Fig. 4 shows much more smooth distribution functions for high stratified clouds. These data were obtained on August 21, 1995 when a thin layer of maritime fog was recorded just above the water surface and a lower cloud field disappeared just before the measurement run of higher clouds. The LCB height was $H = (5424 \pm 223)$ m without any trend. For the distribution $n(H)$, $As = 0.69$, that is, the asymmetry was strong, and the excess coefficient $E = 0.24$ indicated a weakly pronounced flattop peaking. The distribution $n(\varepsilon)$ was similar to $n(H)$ and exhibited the positive coefficient of asymmetry as well.

On the whole, for the above-considered high (according to the classification accepted there) clouds we did not find any trend in the LCB height on our scales, and the fluctuations of the LCB height were $\Delta m = (115 \pm 95)$ m, varying from 11.7 to 264 m. Positive and negative asymmetry coefficients were observed equally often. In the first case, $As = (0.34 \pm 0.31)$, that is, the coefficient of asymmetry was small or moderate. In the second case, $As = -(0.75 \pm 0.42)$, that is, the coefficient of asymmetry was moderate or large. The coefficients of excess were negative, $e = -(1.0 \pm 0.81)$, that is, indicative of the bimodal character of the distribution function. In case of positive coefficient of excess, $e = 1.10 \pm 0.87$.

As to the scattering coefficient at the LCB, we failed to establish any peculiarities for lower and higher clouds. On the whole, $n(\varepsilon_b)$ was, as a rule, asymmetric. The width of the distribution $n(\varepsilon_b)$ at half $\varepsilon_{\rm mod}$ level was $(33 \pm 38)\%$ toward greater values of ε_b. (Once we recorded a shift by 110% from the modal value, that is, the distribution was very smeared but still remained nonuniform.) To the left of $\varepsilon_{\rm mod}$, that is, toward smaller values of ε_b, the width of the distribution $n(\varepsilon_b)$ at half $\varepsilon_{\rm mod}$ was $(41 \pm 17)\%$ of $\varepsilon_{\rm mod}$. The average width of the distribution $n(\varepsilon_b)$ can be written as $\varepsilon_{\rm mod}{}^{+\,0.33\varepsilon_{\rm mod}}_{-\,0.41\varepsilon_{\rm mod}}$. To be objective, we note that up to 10% of experimental data obeyed approximately uniform distribution of ε_b over the entire range of its measured values.

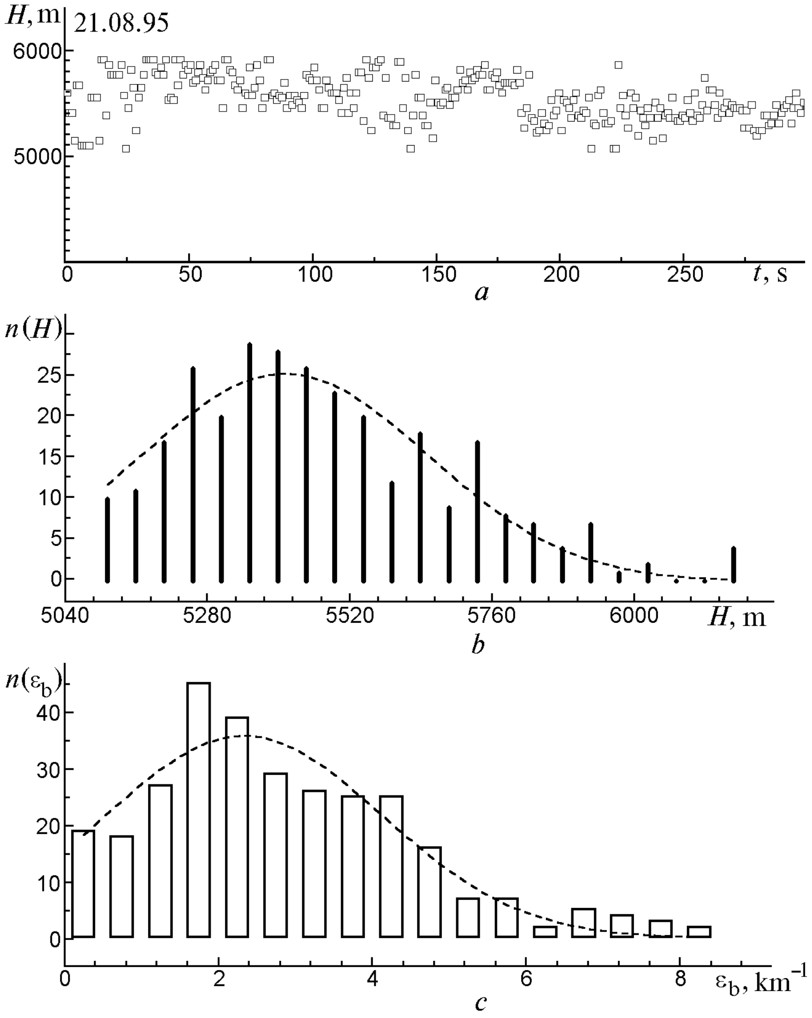

FIG. 4. Sensing of high stratified clouds at 20:58*, ship time on August 8, 1995. Designations are the same as in Fig. 2.*

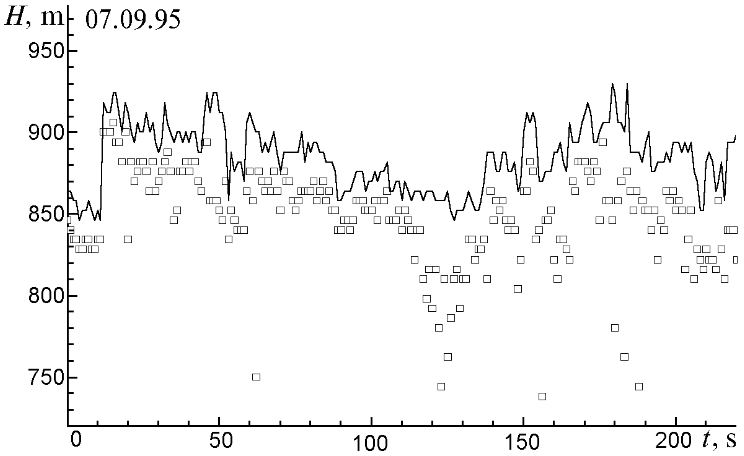

FIG. 5. Profile of the LCB on September 7, 1995. Solid curve is derived by the criterion $r_{\rm m}$ *and small squares – by the criterion* r_0*. Starting from the laser shot No. 110, the lidar sensitivity of an optical channel was increased ten times.*

A fascinating result from the viewpoint of lidar sensing is shown in Fig. 5. In this measurement run, a light filter was removed from a receiving lidar telescope after 110 laser shots. As a result, the sensitivity of photomultipliers increased ten times. But this had practically no effect on the LCB profile determined by the criterion r_m (this is evident from the fluctuations of the solid curve). At the same time, the fluctuations of the LCB height increased several times for the LCB profile derived by the criterion r_0 due to its greater sensitivity. This is evidence in favor of the criterion r_m, which characterizes the cloud in its depth, for a solution of practical problems. However, the parameter r_0, more closely related with transformation of the particle size spectrum at the cloud boundary, can be more useful for a study of the microphysical cloud structure.

Thus, the following generalization can be made. The fluctuations of the lower stratiform cloud boundary height in the North Atlantic most often obey asymmetric distribution rather than the normal one for horizontal scales of 10–70 km. The coefficient of asymmetry may be positive or negative. The radiation extinction coefficient, as a rule, does not obey the normal distribution as well. The elimination of the lower-frequency trend of the LCB height yields less asymmetric distribution.

REFERENCES

1. A.I. Abramochkin, V.V. Zanin, I.E. Penner, et al., Opt. Atm. **1**, No. 2, 92–96 (1988).
2. V.E. Zuev, ed., *Laser Sensing of the Troposphere and the Underlying Surface* (Nauka, Novosibirsk, 1987), 262 pp.
3. S.P. Khramov and L.I. Mamontova, *Meteorological Dictionary* (Gidrometeoizdat, Leningrad, 1963), 620 pp.
4. V.S. Shamanaev, Atmos. Oceanic Opt. **5**, No. 7, 444–447 (1993).
5. A.A. Isaev, *Statistics as Applied to Meteorology and Climatology* (Moscow State University Publishing House, Moscow, 1988), 246 pp.
6. V.P. Leonov, *Experimental Data Processing on Programmable Microcomputers* (Tomsk State University Publishing House, Tomsk, 1990), 376 pp.
7. A.L. Kosarev, I.P. Mazin, A.N. Nevzorov, and V.F. Shugaev, Tr. Tsentr. Aerolog. Observ., No. 124 (1976), 169 pp.